

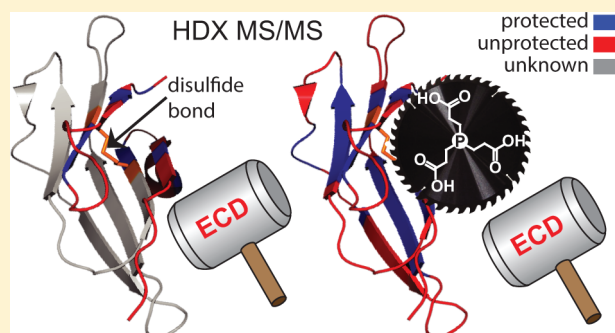
Approach to Characterization of the Higher Order Structure of Disulfide-Containing Proteins Using Hydrogen/Deuterium Exchange and Top-Down Mass Spectrometry

Guanbo Wang[†] and Igor A. Kaltashov*

Department of Chemistry, University of Massachusetts-Amherst, 710 North Pleasant Street, LGRT 104, Amherst, Massachusetts 01003 United States

S Supporting Information

ABSTRACT: Top-down hydrogen/deuterium exchange (HDX) with mass spectrometric (MS) detection has recently matured to become a potent biophysical tool capable of providing valuable information on higher order structure and conformational dynamics of proteins at an unprecedented level of structural detail. However, the scope of the proteins amenable to the analysis by top-down HDX MS still remains limited, with the protein size and the presence of disulfide bonds being the two most important limiting factors. While the limitations imposed by the physical size of the proteins gradually become more relaxed as the sensitivity, resolution and dynamic range of modern MS instrumentation continue to improve at an ever accelerating pace, the presence of the disulfide linkages remains a much less forgiving limitation even for the proteins of relatively modest size. To circumvent this problem, we introduce an online chemical reduction step following completion and quenching of the HDX reactions and prior to the top-down MS measurements of deuterium occupancy of individual backbone amides. Application of the new methodology to the top-down HDX MS characterization of a small (99 residue long) disulfide-containing protein β_2 -microglobulin allowed the backbone amide protection to be probed with nearly a single-residue resolution across the entire sequence. The high-resolution backbone protection pattern deduced from the top-down HDX MS measurements carried out under native conditions is in excellent agreement with the crystal structure of the protein and high-resolution NMR data, suggesting that introduction of the chemical reduction step to the top-down routine does not trigger hydrogen scrambling either during the electrospray ionization process or in the gas phase prior to the protein ion dissociation.



Since its initial introduction in the late 1990s,^{1–3} top-down hydrogen/deuterium exchange (HDX) with mass spectrometric (MS) detection evolved to become a potent biophysical tool capable of providing valuable information on higher order structure and conformational dynamics of proteins at an unprecedented level of structural detail. Among the many advantages offered by top-down HDX MS compared to conventional (bottom-up) measurements are significant reduction or indeed complete elimination of the back exchange,⁴ high spatial resolution,^{5,6} and the ability to study conformational dynamics in the conformer-specific fashion.^{7,8} However, despite the spectacular recent advances and the broader acceptance of this technique, the scope of the proteins amenable to the analysis by top-down HDX MS remains limited, with the protein size and the presence of disulfide bonds being the two most important limiting factors. The limitations imposed by the physical size of the proteins gradually become more relaxed as the sensitivity, resolution, and dynamic range of modern MS instrumentation continue to improve at an ever accelerating pace. However, the presence of disulfides remains a much less forgiving limitation even for the proteins of relatively modest size.

Gas phase cleavage of the disulfide bonds can be achieved using either collision-activated dissociation (CAD) of polypeptide anions^{9–12} or electron-based ion fragmentation techniques.¹³ Unfortunately, collisional activation of peptide and protein ions frequently causes hydrogen scrambling to occur prior to the dissociation event.¹⁴ An additional complication arises due to the fact that the CAD fragments of peptide anions cannot be assigned as readily as those produced upon dissociation of peptide cations, as the two dissociation processes frequently follow very different routes.¹⁵ This effectively rules out negative ion CAD as a robust and efficient tool for top-down HDX MS/MS measurements. On the other hand, electron-based ion fragmentation techniques, such as electron-capture dissociation, ECD,¹³ (and its sister technique, electron transfer dissociation, ETD¹⁶) have been shown to be capable of generating abundant fragment ions without triggering hydrogen scrambling in top-down HDX MS/MS studies.¹⁷ Furthermore, electron-based dissociation techniques

Received: May 13, 2014

Accepted: July 2, 2014

Published: July 2, 2014

are also capable of cleaving disulfide linkages in the gas phase^{18,19} and in fact have been successfully used to separate peptide monomers linked by unreduced disulfide bonds in bottom-up HDX MS measurements.²⁰

Unfortunately, successful application of ECD or ETD to top-down protein sequencing of disulfide-containing proteins requires collisional activation as a necessary step to improve the fragmentation efficiency. ECD or ETD of disulfide-containing protein ions carried out in the absence of collisional heating (to suppress or eliminate hydrogen scrambling) typically result in inferior sequence coverage and low abundance of fragment ions, making dissociation of disulfide linkages in the gas phase poorly suited for HDX MS/MS work. To circumvent this problem, we explore an alternative approach to characterizing the higher order structure of disulfide-containing proteins with top-down HDX MS/MS by introducing online chemical reduction following the quench of HDX reactions. The concentration of the reducing agent is selected such that the adequate reduction of the disulfide bonds can be achieved in solution without causing significant degradation of the protein ion signal in ESI MS (taking advantage of increased tolerance of modern ESI MS instrumentation to the presence of limited amounts of nonvolatile electrolytes in the sprayed solutions). Top-down fragmentation of protein ions with reduced disulfide bonds using ECD allows the distribution of deuterium to be mapped across the entire protein backbone with high spatial resolution. Application of the new methodology to the top-down HDX MS characterization of a small (99 residue long) disulfide-containing protein β_2 -microglobulin allows the backbone amide protection to be probed with nearly a single-residue resolution.

EXPERIMENTAL SECTION

Materials. The recombinant form of β_2 -microglobulin was expressed as an inclusion body in *Escherichia coli* by following the procedure previously described.²¹ Deuterium oxide (99.9% ^2H) was purchased from Cambridge Isotope Laboratories, Inc. (Tewksbury, MA). Ammonium bicarbonate, acetic acid, acetonitrile (HPLC grade), and TCEP were purchased from Fisher Scientific (Pittsburgh, PA).

Hydrogen Exchange. HDX was initiated by mixing a 1 mg/mL protein solution in $^1\text{H}_2\text{O}$ (solution A) with 5 mM ammonium bicarbonate dissolved in $^2\text{H}_2\text{O}$ (solution B) using a previously described home-built continuous-flow apparatus which comprises three inlets and two sequential high-efficiency mixers.⁸ HDX reactions were quenched and the protein molecules were partially reduced using 10 mM TCEP solution in a 1:9 (vol/vol) $^2\text{H}_2\text{O}$ /acetonitrile mixture whose pH was adjusted to 2.5 with formic acid (solution C). Three syringes used to infuse solutions A, B, and C were advanced simultaneously by a single Nexus 300 syringe pump (Chemyx, Inc., Stafford, TX), resulting in a dilution ratio of 1:20 (vol/vol) at the first mixing site and 1:1 (vol/vol) at the second. The second mixing resulted in a 3:20:18 $^1\text{H}_2\text{O}$ / $^2\text{H}_2\text{O}$ /acetonitrile mixture with a final TCEP concentration of 5 mM. Solution C and capillaries downstream of the second mixer were immersed in an ice–water slurry to minimize the possible gain of a ^2H label by the protein past the exchange loop. At the gross flow-rate of 246 $\mu\text{L}/\text{h}$, the lengths of capillaries downstream of the first and second mixers were selected to allow the exchange reactions to proceed for 6 min and the reduction at the HDX quench condition to proceed for ~ 1.5 min, respectively. The

setup was equilibrated for 1 h prior to each measurement. The exchange end-point sample ($\beta_2\text{m}^{**}$) was prepared by collecting the outflow of the setup in a sealed microcentrifuge tube at room temperature for ~ 2 h, followed by 30 min incubation at 40 $^\circ\text{C}$. Measurement of $\beta_2\text{m}^{**}$ was performed on the next day of preparation. As verified by ESI MS, the deuteration of $\beta_2\text{m}^{**}$ was complete.

ESI MS Measurements. ESI MS measurements were carried out with a Solarix (Bruker Daltonics, Billerica, MA) Fourier transform ion cyclotron resonance (FTICR) MS equipped with a 7.0 T superconducting magnet and a standard ESI source, which was directly connected to the outlet of the online mixing apparatus. In MS/MS measurements, protein ions in four successive charge-states (11+ through 14+ for a TCEP-free sample; 14+ through 17+ for a TCEP-treated sample) were mass-isolated in the front-end quadrupole filter followed by electron-capture dissociation (ECD) of precursor ions in the ICR cell of the mass spectrometer. Typically, 2 000–4 000 scans were accumulated for each ECD spectrum to increase the signal-to-noise ratio. Relatively mild ion desolvation and isolation conditions were used to ensure scrambling-free fragmentation of protein ions, as described previously.⁸

HDX MS/MS Data Analysis. Masses of fragment ions were determined as previously described.⁸ The cumulative protection of backbone-amides of a certain segment represented by c- or z-ions was calculated as

$$P(S_k(N)) = \frac{M^{**}(c_{k-1}) - M^*(c_{k-1})}{M(^2\text{H}) - M(^1\text{H})}$$

$$P(S_m(C)) = \frac{M^{**}(z_{m+1}) - M^*(z_{m+1})}{M(^2\text{H}) - M(^1\text{H})}$$

where $P(S_k(N))$ is the total protection of the N-terminal segment spanning residues 1 through k , $P(S_m(C))$ is the total protection of the C-terminal segment spanning residues 100- m through 99, $M(^2\text{H})$ or $M(^1\text{H})$ are the masses of ^2H or ^1H atoms, and $M(c_i)$ or $M(z_i)$ are the masses of c_i or z_i ions. Symbols * and ** represent data of partially exchanged sample and exchange end-point sample, respectively. Amide protection at an individual backbone amide group was determined as

for data deduced from c ions,

$$P(R_i) = P(S_i(N)) - P(S_{i-1}(N))$$

for data deduced from z ions,

$$P(R_i) = P(S_{100-i}(C)) - P(S_{99-i}(C))$$

where $P(R_i)$ is the protection of a backbone amide at residue i . For residues where subsequent fragment ions were missing, $P(R_i)$ was assigned as

for data deduced from c ions,

$$P(R_i) = P(R_{i+1}) = \dots = P(R_{i+j-1}) \\ = \frac{P(S_{i+j-1}(N)) - P(S_{i-1}(N))}{j}$$

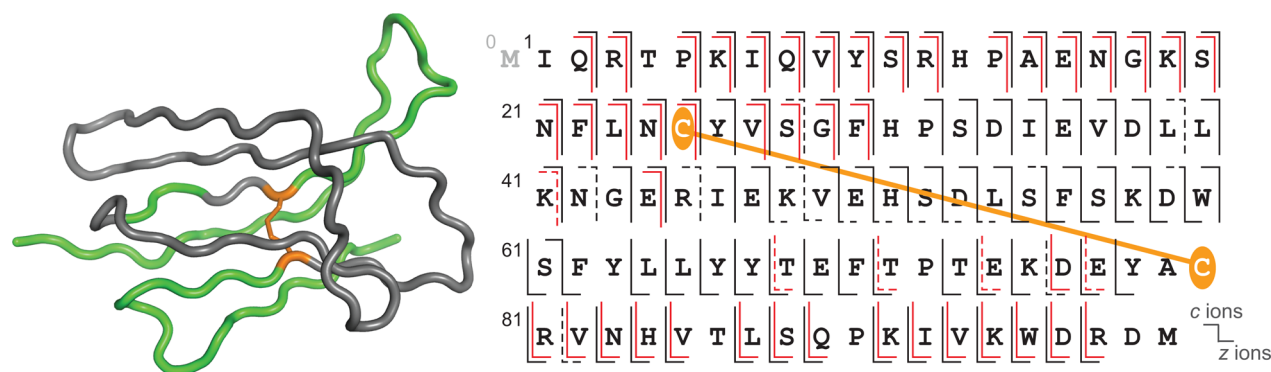


Figure 1. ECD fragmentation patterns of β_2m protein ions generated by ESI from TCEP-free (red) and 5 mM TCEP (black) solutions. Dashed delimiters represent fragments whose ionic signals are not sufficiently abundant to be used in top-down HDX MS measurements (these ions were not used in calculating the sequence coverage). The positions of the two cysteine residues are indicated in orange both within the protein sequence and the tertiary structure of the protein (the gray-colored region shows the protein segment that fails to produce abundant c- and z-ions in the absence of TCEP in solution).

for data deduced from z ions,

$$P(R_i) = P(R_{i+1}) = \dots = P(R_{i+j-1}) \\ = \frac{P(S_{100-i}(C)) - P(S_{100-i-j}(C))}{j}$$

Data analysis was performed using Bruker (Billerica, MA) DataAnalysis, BioTools packages, and Origin Pro 8.5 (Origin Lab, Northampton, MA).

RESULTS AND DISCUSSION

Although ECD is capable of cleaving disulfide linkages in the gas phase,¹⁹ the need to avoid hydrogen scrambling places an additional constraint on experimental conditions by requiring that collisional activation prior to the ECD event be avoided. Collisional heating of protein ions has been shown to be an important (and in many cases critical) accessory to ECD, as it provides internal energy necessary for physical separation of fragment ions produced by ECD.²² The enhancement of the ECD yields by collisional heating is particularly noticeable for protein ions produced under near-native conditions, as it disrupts the network of hydrogen bonds (many of which survive transition from solution to the gas phase) that may otherwise prevent physical separation of protein fragments produced by the backbone cleavages. Although the complex and highly organized network of native hydrogen bonds is unlikely to survive acidification of the protein solution (which is used to quench the exchange reactions prior to MS measurements), disulfide-containing proteins are likely to be an exception, as the conformational constraints introduced by the cross-chain disulfide linkages can (and frequently do) reinforce the residual structure even under denaturing conditions.^{23–25}

ECD of unlabeled β_2m placed in an acidic quench solution gives rise to abundant c- and z-fragment ions even in the absence of collisional heating of the protein ions. However, a detailed examination of this set of fragment ions reveals that nearly all of them are derived from the N- and C-terminal segments of the protein before and after the two cysteine residues connected by the disulfide bond (Figure 1), with very few of the observed fragments representing backbone cleavages within the (Cys²⁵–Cys⁸⁰) segment. In fact, even though complete sequence coverage at near-single residue resolution

is achieved outside the disulfide-bridged region, the scarcity of the structurally diagnostic ions derived from the (Cys²⁵–Cys⁸⁰) segment suggests that ECD of both the disulfide bond and backbone N–C(α) bonds under conditions minimizing hydrogen scrambling cannot be effectively used in topdown HDX MS measurements.

The common approach to reducing disulfide bonds in bottom-up HDX MS measurements is to use a reducing agent that remains at least partially active under the acidic (slow exchange) conditions, such as tris(2-carboxyethyl)phosphine (TCEP).²⁶ Upon completion of the proteolytic step, TCEP and its oxidized form are removed from the sample during the fast LC step. However, this approach cannot be used in the top-down HDX MS measurements, which almost always utilize direct infusion of the protein solution to the ESI source to increase the data acquisition window and do not allow the desalting step to be introduced prior to protein ionization.

Although TCEP is a weak acid (with the pK_a values ranging from 2.9 to 7.7²⁷), the presence of a basic site (ternary phosphorus) alongside three acidic ones (carboxylic groups) makes it an ionic compound at any pH (even the electrically neutral species of TCEP being a zwitterion). The ionic character of TCEP in solution makes it behave in a fashion similar to strong electrolytes vis-à-vis influencing the quality of ESI mass spectra of protein solutions containing such species: the degradation of the quality is caused both by highly abundant ionic signals of the electrolytes and their clusters and by forming multiple adducts of protein ions.^{28,29} Nevertheless, continuous improvements in the design of commercial ESI sources have made them noticeably more tolerant to the presence of moderate amounts of strong nonvolatile electrolytes; in fact, it is now possible to obtain abundant signal of relatively large proteins in ESI MS of solutions containing low millimolar quantities of NaCl and other nonvolatile salts.³⁰ This prompted us to evaluate the feasibility of using moderate amounts of TCEP as a reducing agent in top-down HDX MS measurements without removing it from the protein solution prior to the ESI step.

The presence of 5 mM TCEP in the $\sim 2 \mu M$ solution of β_2m at pH 2.5 does give rise to the ionic peaks representing TCEP clusters as well as the oxidized form of TCEP (P-oxide, TCEPO), but their overall abundance is comparable to that of the protein ions (Figure 2). Furthermore, formation of the protein-TCEP adducts is negligible under these conditions.

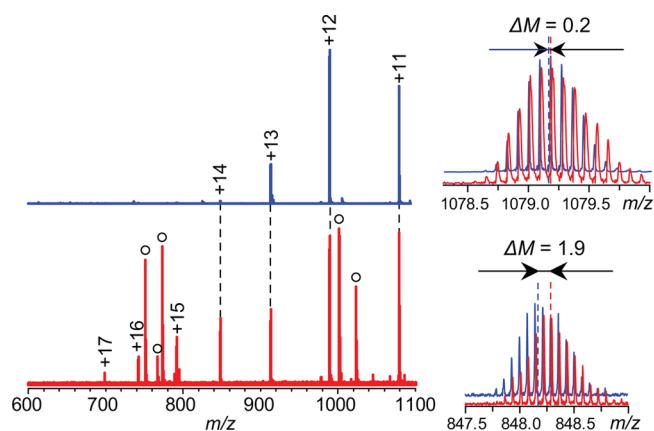


Figure 2. ESI mass spectra of 2 μM $\beta_2\text{m}$ in TCEP-free (blue) and 5 mM TCEP-containing (red) quench solutions. Peaks labeled with circles correspond to TCEP and TCEPO clusters. The two side panels show isotopic distributions of protein ions at charge states 11+ and 14+ generated from TCEP-free (blue) and TCEP-containing (red) solutions.

Complete reduction of the disulfide bridge in $\beta_2\text{m}$ could not be achieved using such a relatively modest amount of TCEP in the protein solution and suboptimal conditions (low pH and temperature), as suggested by the appearance of the isotopic distributions of peaks representing $\beta_2\text{m}$ ions at charge states 12+ and lower (Figure 2). At the same time, the mass spectrum contains abundant protein ion peaks at higher charge density (up to 17+), which have not been observed or had very low abundance in the TCEP-free solution of this protein. Isotopic distributions of these ions clearly indicate that the disulfide bond is reduced (mass shift by 2 units, see Figure 2).

The emergence of this population of relatively high charge density protein ions with reduced cysteine residues provides

multiple benefits vis-à-vis the top-down HDX MS measurements. First, the increased charge on the protein ion makes the electron capture process more efficient by increasing the effective cross-section of the electron–polycation interaction.³¹ Furthermore, increase of the protein ion charge state indicates loss of compactness in solution³² (triggered by the elimination of the constraint imposed by the disulfide bond), making it highly unlikely that the conformation of these proteins in the gas phase will have native-like hydrogen bonds that would prevent physical separation of the protein ion fragments produced by fission of the backbone. Indeed, ECD of the $\beta_2\text{m}$ ions generated by ESI of the TCEP-containing solution of this protein results in facile cleavages of most of the N–C(α) bonds across the entire protein sequence, including the (Cys²⁵–Cys⁸⁰) region (Figure 1). Overall, 80 abundant c- or z-ions are observed in the ECD spectrum, providing a 70% coverage of the protein sequence at single-residue resolution with an additional 22% of the sequence covered at two-residue resolution. The large number of fragment ions results in spectral congestion, leading to partial overlaps of isotopic distributions of some fragment ions; in most cases these overlaps can be resolved (see the Supporting Information for more detail).

The cumulative protection maps of backbone amides within the N- and C-terminal segments of the protein (calculated based on the measured deuterium content of either c- or z-fragment ions generated by ECD of the $\beta_2\text{m}$ ions produced by ESI of the protein solution where the amide exchange was quenched and the disulfide bridges partially reduced by TCEP) show a very uneven distribution of amide protection across the protein backbone (Figure 3, top). A more intuitive presentation of these data shows protection levels of individual backbone amides, which were calculated for each residue by subtracting the deuterium content of adjacent fragments in either the c- or

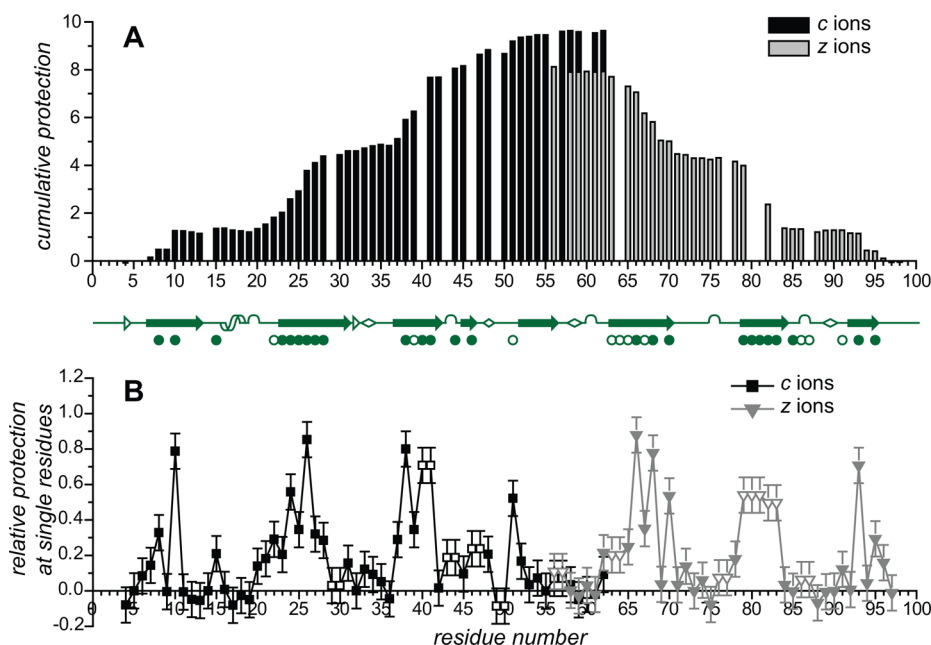


Figure 3. Cumulative (top) and residue-level (bottom) protection patterns of $\beta_2\text{m}$ derived from the top-down HDX MS measurements. Black and gray bars/symbols represent data obtained from c- ions and z-ions, respectively. Open symbols in the bottom diagram represent data where single-residue resolution was not available. Secondary structural elements of native $\beta_2\text{m}$ (PDB ID: 1LDS) are shown schematically between the two graphs using a standard PDB line notation (with diamond as an additional symbol which represents a bend). Open and closed circles indicate residues whose backbone amide ^1H labels were still retained after 40 min and 22 h of exchange, respectively, as measured by NMR.³⁴

z-ladder (Figure 3, bottom). The absolute value of the most negative $P(R_i)$ (0.1) was treated as the extreme value of error oscillation, and any residue R_i where the value of $P(R_i)$ exceeded 0.2 (the double of 0.1) was regarded as a residue having significant protection. This protection map is generally in good agreement with the secondary structure of β_2m (shown in Figure 3 using line notations) deduced from the X-ray crystal structure of this protein,³³ although some discrepancy does exist. For example, relatively low protection was observed for most residues comprising β -strand 4 (residues S2–S5), while noticeable protection was detected at residue S1, which immediately precedes this strand. In order to understand the origin of this anomaly, top-down HDX MS data were compared with the protection factors derived from previously reported high-resolution NMR measurements.³⁴ The NMR-derived protection data (which are usually considered to be a better representation of dynamic structures of proteins in solution) are also mapped on the β_2m sequence in Figure 3 and clearly show that several β -strand of this protein are noticeably dynamic. In fact, no protection is detected within the residues comprising β -strand 5, with strand 1 also showing highly dynamic character. Overall, there is a remarkable agreement between the backbone protection patterns derived from the high-resolution NMR and top down HDX MS measurements. Disagreements between the two data sets exceeding the experimental error were noted for only a few residues (e.g., Glu⁴⁴, Glu⁴⁷, and Val⁸⁵) and are likely caused by difference in solution conditions (such as pH, buffer makeup, ionic strength, and temperature) and expectedly by spatially unresolved residues' splitting their total deuterium contents. It might also be possible that some of the isotopic distributions of β_2m fragment ions produced by cleavages of the backbone outside of the protein segment between the two cysteine residues may have contributions from the oxidized form of the protein. This would introduce a change in the apparent deuterium content by shifting the fragment ion mass. However, the contribution of the oxidized (disulfide-intact) species to the pool of fragment ions representing the backbone cleavage between the two cysteine residues is negligible (see Figure 1), while the masses of fragment ions produced by cleavages of the backbone outside of this segment do not depend on the oxidation state of the cysteine residues. The excellent agreement between the backbone protection patterns of β_2m derived from the top-down HDX MS and high-resolution NMR measurements clearly suggests that hydrogen scrambling does not occur during or prior to the ECD fragmentation of the protein ions.

CONCLUSIONS

In this work we demonstrated feasibility of applying top-down HDX MS measurements to characterize higher order structure and conformational dynamics of disulfide-containing proteins, which have been out of the reach of this technique so far. Use of a moderate amount of a reducing agent TCEP is compatible with the ESI process, while allowing a fraction of the protein molecules to be reduced in solution thereby enabling near-complete sequence coverage at high resolution. The agreement between the top-down HDX MS and NMR data sets demonstrate that the new experimental approach is capable of capturing the dynamic picture of protein conformation at high spatial resolution without compromising the quality of the data by triggering hydrogen scrambling in the gas phase. Despite its modest size, β_2m is known to be able to populate a non-native state,³⁵ which might be a key player in a variety of

processes, including amyloidosis. However, the structure of this non-native state of β_2m remains elusive since this conformer exists in dynamic equilibrium with the native state of the protein.^{36,37} Recently we demonstrated that top-down HDX MS provides an elegant way to selectively probe structure of protein states coexisting in solution at equilibrium;⁸ however, β_2m remained out of reach of this technique until recently due to the presence of a disulfide bond. The ability to expand the scope of top-down HDX MS to disulfide-containing proteins opens up a host of exciting possibilities to explore the structure of β_2m , interferon, lysozyme, and a variety of other disulfide-containing proteins in a conformer-specific fashion, where physiologically important non-native states may play important roles in processes as diverse as folding, recognition, signaling, and amyloidosis.

ASSOCIATED CONTENT

Supporting Information

Representative examples of isotopic distributions of fragment ions that have (Supplementary Figure 1) and have not (Supplementary Figure 2) been used to calculate the deuterium occupancy at individual backbone amides of β_2m in top-down HDX MS measurements. This material is available free of charge via the Internet at <http://pubs.acs.org>.

AUTHOR INFORMATION

Corresponding Author

*Phone: (413) 545-1460. Fax: (413) 545-4490. E-mail: Kaltashov@chem.umass.edu.

Present Address

[†]Guanbo Wang: Biomolecular Mass Spectrometry and Proteomics Group, Bijvoet Center for Biomolecular Research and Utrecht Institute for Pharmaceutical Sciences, Utrecht University, Padualaan 8, 3584 CH Utrecht, The Netherlands.

Notes

The authors declare no competing financial interest.

ACKNOWLEDGMENTS

This work was supported by the NIH Grant R01 GM061666. The authors are grateful to Prof. Ersilia De Lorenzi (University of Pavia, Italy) for inspiring this work and for useful discussion. The FTICR mass spectrometer has been acquired through the Major Research Instrumentation Grant CHE-0923329 from the National Science Foundation. We also thank Dr. Rinat R. Abzalimov (UMass-Amherst) for helpful discussion and Dr. Cedric E. Bobst (UMass-Amherst) for help with the initial design of the HDX apparatus and preparation of manuscript.

REFERENCES

- (1) Eyles, S. J.; Dresch, T.; Gierasch, L. M.; Kaltashov, I. A. *J. Mass Spectrom.* **1999**, *34*, 1289–1295.
- (2) Akashi, S.; Naito, Y.; Takio, K. *Anal. Chem.* **1999**, *71*, 4974–4980.
- (3) Eyles, S. J.; Speir, J. P.; Kruppa, G. H.; Gierasch, L. M.; Kaltashov, I. A. *J. Am. Chem. Soc.* **2000**, *122*, 495–500.
- (4) Kaltashov, I. A.; Bobst, C. E.; Abzalimov, R. R. *Anal. Chem.* **2009**, *81*, 7892–7899.
- (5) Pan, J. X.; Han, J.; Borchers, C. H.; Konermann, L. *J. Am. Chem. Soc.* **2009**, *131*, 12801–12808.
- (6) Pan, J. X.; Han, J.; Borchers, C. H.; Konermann, L. *Anal. Chem.* **2010**, *82*, 8591–8597.
- (7) Pan, J. X.; Han, J.; Borchers, C. H.; Konermann, L. *Anal. Chem.* **2011**, *83*, 5386–5393.

- (8) Wang, G. B.; Abzalimov, R. R.; Bobst, C. E.; Kaltashov, I. A. *Proc. Natl. Acad. Sci. U.S.A.* **2013**, *110*, 20087–20092.
- (9) Chrisman, P. A.; McLuckey, S. A. *J. Proteome Res.* **2002**, *1*, 549–557.
- (10) Bilusich, D.; Maselli, V. M.; Brinkworth, C. S.; Samguina, T.; Lebedev, A. T.; Bowie, J. H. *Rapid Commun. Mass Spectrom.* **2005**, *19*, 3063–3074.
- (11) Bilusich, D.; Bowie, J. H. *Rapid Commun. Mass Spectrom.* **2007**, *21*, 619–628.
- (12) Zhang, M. X.; Kaltashov, I. A. *Anal. Chem.* **2006**, *78*, 4820–4829.
- (13) Zubarev, R. A. *Curr. Opin. Biotechnol.* **2004**, *15*, 12–16.
- (14) Abzalimov, R. R.; Kaltashov, I. A. *Anal. Chem.* **2010**, *82*, 942–950.
- (15) Bowie, J. H.; Brinkworth, C. S.; Dua, S. *Mass Spectrom. Rev.* **2002**, *21*, 87–107.
- (16) Syka, J. E. P.; Coon, J. J.; Schroeder, M. J.; Shabanowitz, J.; Hunt, D. F. *Proc. Natl. Acad. Sci. U.S.A.* **2004**, *101*, 9528–9533.
- (17) Abzalimov, R. R.; Kaplan, D. A.; Easterling, M. L.; Kaltashov, I. A. *J. Am. Soc. Mass Spectrom.* **2009**, *20*, 1514–1517.
- (18) Zubarev, R. A.; Kruger, N. A.; Fridriksson, E. K.; Lewis, M. A.; Horn, D. M.; Carpenter, B. K.; McLafferty, F. W. *J. Am. Chem. Soc.* **1999**, *121*, 2857–2862.
- (19) Ganisl, B.; Breuker, K. *ChemistryOpen* **2012**, *1*, 260–268.
- (20) Bobst, C. E.; Kaltashov, I. A. *Anal. Chem.* **2014**, *86*, 5225–5231.
- (21) Esposito, G.; Michelutti, R.; Verdone, G.; Viglino, P.; Hernandez, H.; Robinson, C. V.; Amoresano, A.; Dal Piaz, F.; Monti, M.; Pucci, P.; Mangione, P.; Stoppini, M.; Merlini, G.; Ferri, G.; Bellotti, V. *Protein Sci.* **2000**, *9*, 831–845.
- (22) Breuker, K.; Oh, H. B.; Lin, C.; Carpenter, B. K.; McLafferty, F. W. *Proc. Natl. Acad. Sci. U.S.A.* **2004**, *101*, 14011–14016.
- (23) Robinson, E. W.; Sellon, R. E.; Williams, E. R. *Int. J. Mass Spectrom.* **2007**, *259*, 87–95.
- (24) Gross, D. S.; Schnier, P. D.; RodriguezCruz, S. E.; Fagerquist, C. K.; Williams, E. R. *Proc. Natl. Acad. Sci. U.S.A.* **1996**, *93*, 3143–3148.
- (25) Valentine, S. J.; Anderson, J. G.; Ellington, A. D.; Clemmer, D. E. *J. Phys. Chem. B* **1997**, *101*, 3891–3900.
- (26) Burns, J. A.; Butler, J. C.; Moran, J.; Whitesides, G. M. *J. Org. Chem.* **1991**, *56*, 2648–2650.
- (27) Krężel, A.; Latajka, R.; Bujacz, G. D.; Bal, W. *Inorg. Chem.* **2003**, *42*, 1994–2003.
- (28) Cech, N. B.; Enke, C. G. *Mass Spectrom. Rev.* **2001**, *20*, 362–387.
- (29) Griffith, W. P.; Mohimen, A.; Abzalimov, R. R.; Kaltashov, I. A. Characterization of Protein Higher Order Structure and Dynamics with ESI MS. In *Protein Mass Spectrometry*; Whitelegge, J. P., Ed.; Comprehensive Analytical Chemistry, Vol. 52; Elsevier: Amsterdam, The Netherlands, 2008; pp 47–62.
- (30) Abzalimov, R. R.; Bobst, C. E.; Salinas, P. A.; Savickas, P.; Thomas, J. J.; Kaltashov, I. A. *Anal. Chem.* **2013**, *85*, 1591–1596.
- (31) Iavarone, A. T.; Paech, K.; Williams, E. R. *Anal. Chem.* **2004**, *76*, 2231–2238.
- (32) Kaltashov, I. A.; Abzalimov, R. R. *J. Am. Soc. Mass Spectrom.* **2008**, *19*, 1239–1246.
- (33) Trinh, C. H.; Smith, D. P.; Kalverda, A. P.; Phillips, S. E. V.; Radford, S. E. *Proc. Natl. Acad. Sci. U.S.A.* **2002**, *99*, 9771–9776.
- (34) Villanueva, J.; Hoshino, M.; Katou, H.; Kardos, J.; Hasegawa, K.; Naiki, H.; Goto, Y. *Protein Sci.* **2004**, *13*, 797–809.
- (35) Chiti, F.; Mangione, P.; Andreola, A.; Giorgetti, S.; Stefani, M.; Dobson, C. M.; Bellotti, V.; Taddei, N. *J. Mol. Biol.* **2001**, *307*, 379–391.
- (36) Chiti, F.; De Lorenzi, E.; Grossi, S.; Mangione, P.; Giorgetti, S.; Caccialanza, G.; Dobson, C. M.; Merlini, G.; Ramponi, G.; Bellotti, V. *J. Biol. Chem.* **2001**, *276*, 46714–46721.
- (37) Bertolotti, L.; Regazzoni, L.; Aldini, G.; Colombo, R.; Abballe, F.; Caccialanza, G.; De Lorenzi, E. *Anal. Chim. Acta* **2013**, *771*, 108–114.